ESD-TR-87-014

Project Report
ETS-78

Zoom vs Full-Field Sensitivity at the ETS

L.G. Taff
D.M. Jonuskis

17 September 1987

Lincoln Laboratory
MASSACHUSETTS INSTITUTE OF TECHNOLOGY
LEXINGTON, MASSACHUSETTS

Prepared for the Department of the Air Force
under Electronic Systems Division Contract F19628-85-C-0002.

The work reported in this document was performed at Lincoln Laboratory, a center for research operated by Massachusetts Institute of Technology, with the support of the Department of the Air Force under Contract F19628-85-C-0002.

This technical report has been reviewed and is approved for publication.

FOR THE COMMANDER

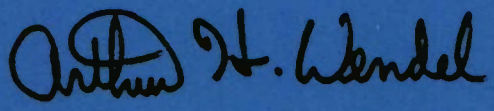

Arthur H. Wendel, Captain, USAF
Acting Chief, ESD Lincoln Laboratory Project Office

MASSACHUSETTS INSTITUTE OF TECHNOLOGY
LINCOLN LABORATORY

ZOOM VS FULL-FIELD SENSITIVITY AT THE ETS

L.G. TAFF
D.M. JONUSKIS
Group 94

PROJECT REPORT ETS-78

17 SEPTEMBER 1987

LEXINGTON MASSACHUSETTS

ABSTRACT

This report discusses a formal attempt to quantify the zoom vs full-field sensitivities of the EBSICON cameras at the Experimental Test System of the Ground-based Electro-Optical Deep Space Surveillance (GEODSS) network. Our results are inconclusive owing to lack of data. The hypothesis that the electronically zoomed configuration can reach approximately $0^{m}.5$ fainter than the full-field mode neither can be confirmed nor denied on the basis of our work. More testing of these devices, and a wider variety of testing in general, is needed.

TABLE OF CONTENTS

LIST OF ILLUSTRATIONS

LIST OF TABLES

ZOOM vs FULL-FIELD SENSITIVITY AT THE ETS

I. BACKGROUND

Over the course of the last several years observing roles played by the Experimental Test System (ETS) have expanded from deep-space artificial satellite surveillance and Earth-approaching asteroid searches to encompass daytime observations of near-Earth satellites and searches for debris in near-Earth orbit. The latter work is performed at twilight while the first two occur in full darkness. This range of observing conditions from sunlight sky to darkest moonless nights, coupled with an angular speed range of a couple degrees/day to 5°/sec (432,000°/day), stretches old observing procedures, calibration techniques, and data reduction methods. New ones (Taff, 1985; Yakutis, Taff, and Sayer, 1986; Taff, 1986) need to be invented to supplement standard practices.

We are attempting to solve a long-standing problem in real-time photometry: How to recover a meaningful apparent magnitude from the occurrence of a streak observed with the ETS cameras. Responsivity is that of an S-20 photo-surface. We prefer that the magnitude be in a standard astronomical system. The purpose of reliably and repeatedly being able to obtain an apparent magnitude is to utilize it in an attempt to deduce size information about the object responsible for the streak.

So far we have been unsuccessful. In our attempts to divine the causes of our repetitive failures we have been forced to question our operating assumptions with regard to the electron-bombarded, silicon-diode, low-light-level cameras at the ETS. We have discovered that the performance characteristics of the cameras have not been documented fully, many tests of the camera systems that should have been carried out were not, and the cameras do not function simply. This report concentrates on the issue of sensitivity in full-field vs zoom configuration. "Canonical knowledge" maintains that sensitivity in the electronically zoomed field of view is higher (better) than in the nominal full-field configuration. We know of no concrete evidence to support this assertion. We doubted it based upon some informal tests we conducted and therefore set out to test this hypothesis. This issue and our previous difficulties bring to mind several experiments that should be performed on the ETS cameras to characterize scintillations, sensitivity, responsivity, color corrections to a standard astronomical system, optimum field of view for a given signal-to-noise ratio, and so on. Each one of these topics can be unexpectedly complex — as an example consider scintillations: How many are there per frame? Where do they occur? Is this distribution radial? What is the lightcurve of a typical scintillation? How long does a typical scintillation last? What is the areal extent and morphological nature of a typical scintillation? Does this vary with time? What does the distribution of maximum amplitudes look like? Why? And so forth.

II. SENSITIVITY

It has long been said that the sensitivity of the ETS cameras was better in the 2:1 zoom mode than in full-field. The difference was $\sim 0^{m}.5$. We set out to test this claim.

We immediately rejected, as an acceptable empirical test, the ability to see a particular light source, such as a star, on the video display monitors. The main problem with this type of observing is that one is preconditioned to expect a certain result. After all, one would be looking for *a* particular star to be visible at *a* particular place when one knows (from the finding chart) that in fact the star is really there (that is, on the sky). In addition, this method is not quantitative.

Another drawback of this type of procedure is that, at best, it provides a point comparison between the two fields of view. In more generalized detection or search problems it is the average sensitivity that is of interest. Thus, we want not only a quantitative measure but we want to incorporate as many point measurements as possible in order to approach an "average sensitivity" for a field of view.

We already had available to us a set of point signal-to-noise measurements (performed with one star) from which we could make rough isophotal contour maps. These are reproduced in Figure I. (The ETS is a duplex facility with two telescope/camera combinations known as A and B.) Judging from the topology of these plots, we fixed on a 16-point, equally spaced grid as adequate to provide realistic estimates for a configuration's average sensitivity. Unfortunately, bad weather during the time scheduled for the acquisition of this data forced us to reduce our set to that shown in Figure 2. It has only 8 points per field of view.

Next we had to choose a quantitative measure of sensitivity. We decided that a measurement of signal-to-noise ratio would be intuitively accessible to a wider audience than a value of limiting magnitude. The signal-to-noise ratio also incorporates a measure of the night-sky background in an integral fashion.

Our method of obtaining the intensity levels necessary for the signal-to-noise ratio is simple. We availed ourselves of the new presence of a VICOM Systems, Inc. Model 1800 digital image processor. One of the preprogrammed capabilities of this device is to print out an 8×8 array of pixel intensities. This box may be located anywhere across the 512×512 digital video format via a trackball. Software was written to transfer these 64 intensity values onto magnetic tape. The tapes were returned to Lincoln Laboratory for further processing.

As explained in detail in Section IV, these 64-element intensity arrays, including their morphology, were used to deduce a value for the average background signal level and the total value of the star plus background signal level in those N pixels believed to contain starlight. If B represents the total background level and S is the total signal count from all pixels containing starlight, then the signal-to-noise ratio is just

$$\frac{S - NB/(64 - N)}{\sqrt{S}} \quad . \tag{1}$$

The derivation of this equation is discussed at the end of Section IV.

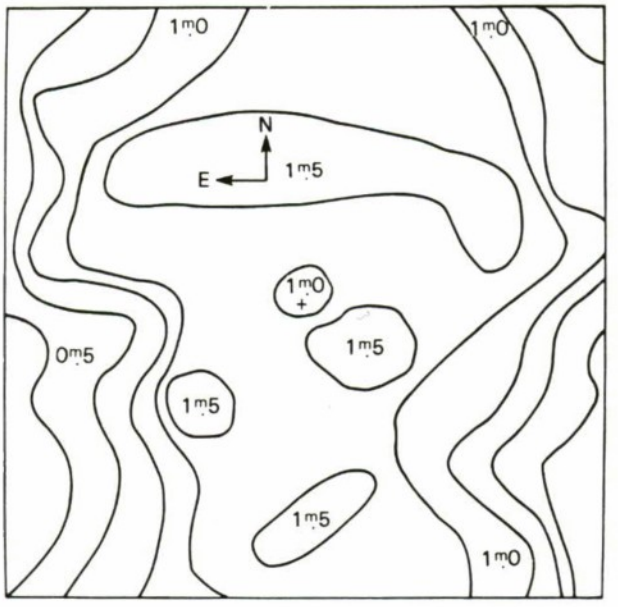

(a)

79177-1

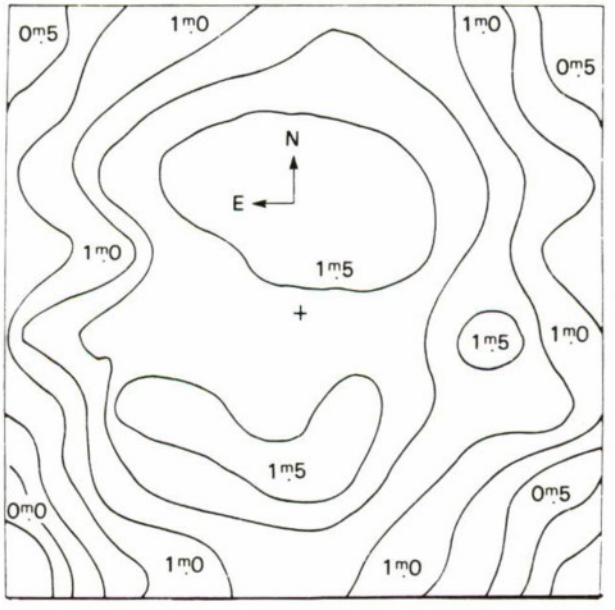

(b)

79177-2

Figure 1. (a) Isophotal contour map of the A-EBSICON camera at the ETS. The maximum sensitivity is near the center. It falls off radially in a roughly circularly symmetric fashion. (b) Same as (a) but for the B-EBSICON camera.

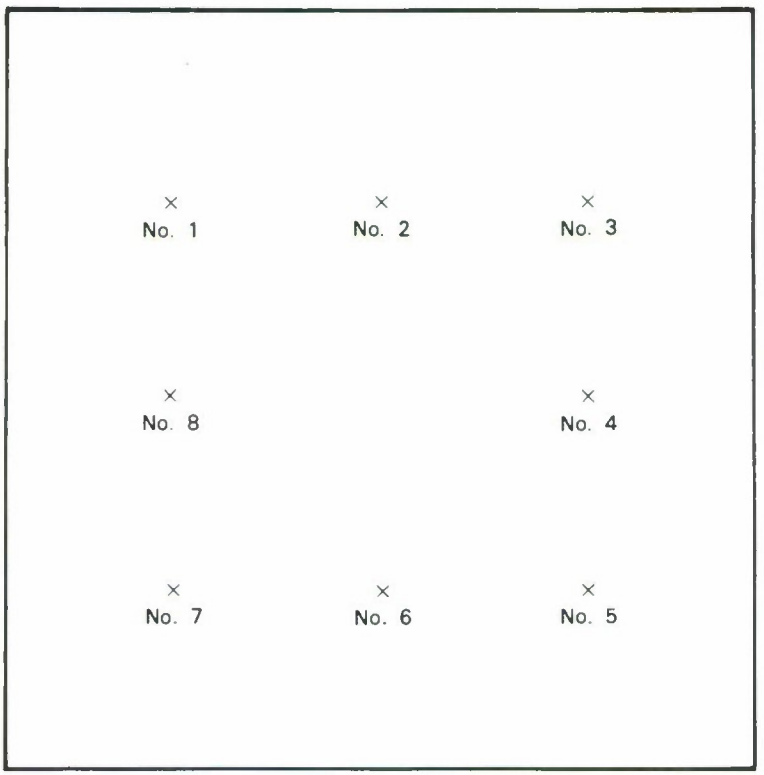

79177-3

Figure 2. Actual locations of central positions for sensitivity testing. Drawn to scale.

III. SELECTION OF STELLAR STANDARDS

We have two methods to experimentally determine signal-to-noise ratios. We either observe a calibrated light source or stars of known brightness and color index. A calibrated light source sounds attractive but is not practical. Hence, we devoted effort to finding an appropriate star field. As it is best to perform the observations as quickly as possible (to minimize atmospheric transparency variations) and with minimum telescope movement (both to mitigate against the camera's lack of shielding from the Earth's magnetic field and viewing through different parts of the atmosphere), one is forced to look for a star field of small angular extent with good photometry. This means either a standard calibration field or a star cluster. Given the time of year when the observations were scheduled and the desire to remain as close to the astronomical zenith as possible (once again to minimize atmospheric corruption of the data), the choice rapidly diminished to the open cluster Praesepe (= M44 = NGC2632). The cluster's center is near 8^h45^m, +21°. The photometry was taken from a recent proper motion study by Jones and Cudworth (1983). We have reproduced their finding chart as Figure 3.

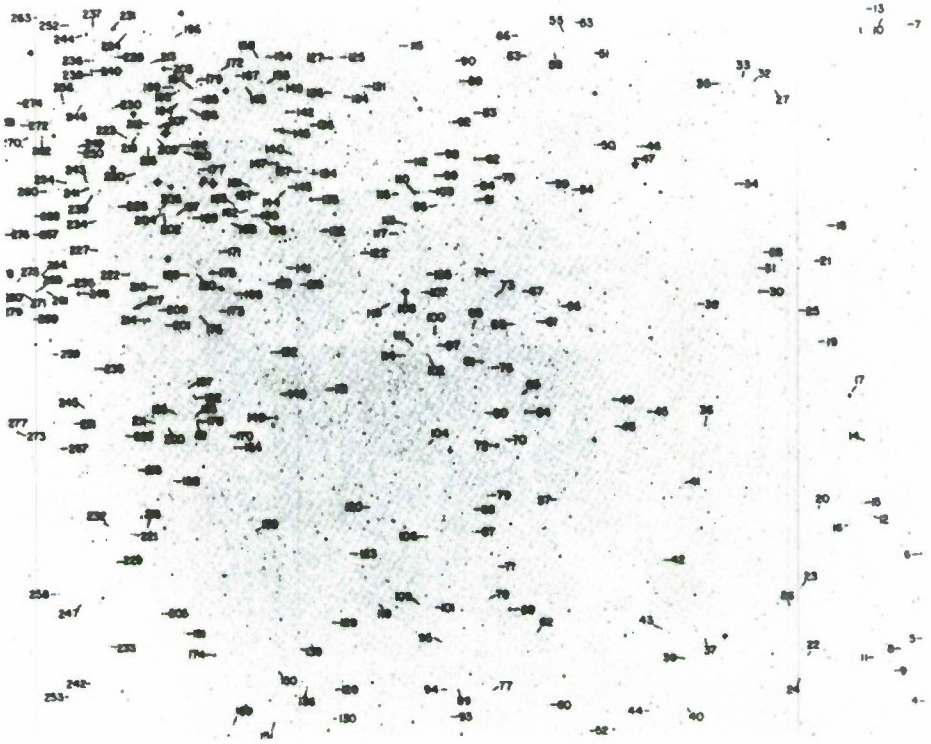

79177-4

Figure 3. Finding chart taken from Jones and Cudworth (1983). North is up, East is to the left. The numbers refer to their internal numbering system.

Note that a globular cluster would be unsuitable for this task because the areal density of stars therein is so high that we would have difficulty obtaining only one star in our 8×8 array ($\simeq 65'' \times 65''$ in full field). Conversely, traditional calibration fields, such as Selected Areas, are generally so sparsely investigated that a variety of potential candidates would be lacking. This is important because we want the narrowest possible color index range for our stars. Until and unless both the camera target's color responsivity is thoroughly examined and the extant $B,V \rightarrow m_{20}$ relationship reinvestigated (Sorvari, 1977), the possibility of the vitiation of our results exists. This is because our chosen stars are not as bright (or as faint) to an S-20 photo-surface as we think they are if we have the incorrect $B,V \rightarrow m_{20}$ formula. Clearly, if our stars are of a different brightness than they are believed to be owing to this problem, then the calibration of signal-to-noise measurements will be systematically biased. As it is, the color index range in Table 1 is uncomfortably large. An alternate source of systematic error would be if the EBSICON photo-surface did not have a true S-20 responsivity.

TABLE I

Star Magnitudes and Colors

Star Number	V	B-V	m_{20}
118	$11^m.83$	$+0^m.79$	$11^m.93$
237	$13^m.46$	$+1^m.29$	$13^m.87$
125	$13^m.89$	$+1^m.39$	$14^m.36$
185	$14^m.53$	$+0^m.85$	$14^m.67$
167	$15^m.19$	$+1^m.51$	$15^m.73$
148	$16^m.05$	$+1^m.58$	$16^m.63$

IV. STAR-FINDING ALGORITHM

Figure 4(a) shows one 8×8 pixel intensity array we gathered. The star shows up quite clearly as the cluster of high signal levels near the center. The intensity counts far from the stellar core are nearly constant and much lower in amplitude. Where, *exactly*, does the star end and the background begin? For Figure 4(a) the decision is not too hard to make, but for Figure 4(b) it is. Therefore, and in light of the other camera calibration work that clearly needs to be performed, we invested some time and effort into inventing an algorithm to automate this decision-making process. In addition, because we know a fair amount about stellar "images" obtained by these cameras, we made the algorithm smart.

We know that no 8×8 array is empty, contains more than one star, nor has more than half its 64 pixels lit by starlight. This knowledge is the result of positioning the telescope carefully, placing the 8×8 box even more carefully, and looking at each of the 8×8 maps we recorded. We also know that the electron read beam sweeps from left to right and from top to bottom. The phenomenon of beam stealing or blooming causes stellar images to be roughly elliptical. The major axis tilts up and to the left. Finally, there is a definite overflow phenomenon on the video scan line containing the brightest pixel. This causes pixels to its right to be exceptionally bright. All this information, plus the fact that stellar images are closed and compact, went into designing the algorithm.

We start by imbedding the 8×8 intensity arrays into 10×10 pseudo-intensity arrays. The existence of the border simplifies the design of our logic. We find the amplitude level of the 32nd faintest pixel and assign all the original 64 pixels at or below this signal level to the background category. Next we compute the mean μ and standard deviation about the mean σ for this intensity-biased background subset. All the border pixels have their intensities set equal to μ. We use as a threshold the larger of $\mu + 3\sigma$ and the intensity level of the 32nd faintest pixel.

Next we find the brightest pixel. This is at the core of the stellar image. We assign it to be a star pixel and examine each of its 8-connected neighbors, as shown in Figure 5(a). If any of these pixels has an intensity level above the threshold it is assigned to be a star pixel, otherwise it is left unassigned as are many of the remaining pixels (at this point).

We now begin an iterative process of trying to grow the subregion of the original 3×3 array assigned to be stellar. At each step we construct the perimeter of the star and compute the mean and standard deviation of the intensity level therein (μ_p, σ_p). All pixels not designated as stellar or perimeter are now temporarily assigned to be background pixels. The mean (μ_b) and standard deviation about the mean (σ_b) for this subset of the entire 10×10 array is calculated. This information is used to answer the query: Is μ_p significantly greater than μ_b? If the answer is yes (at some high confidence level such as 95 percent), then the perimeter must contain pixels which are illuminated by starlight. If the answer is no, then the perimeter pixels are all truly background pixels and the star image has been defined completely.

UPPER LEFT

27	28	28	27	29	27	27	28
26	27	28	30	30	28	28	27
28	28	33	41	41	34	30	28
30	30	43	73	71	48	37	31
31	31	38	64	69	49	36	30
27	27	29	33	36	32	30	28
28	27	28	28	28	28	29	28
28	27	26	28	27	27	28	27

(a)

LOWER RIGHT

79177-5

UPPER LEFT

29	29	28	29	30	29	29	30
31	31	31	32	31	31	31	31
32	31	34	40	40	34	32	32
34	33	39	72	71	45	40	35
33	33	38	61	62	42	37	34
33	32	33	35	35	34	32	32
33	31	31	31	31	32	31	32
33	32	31	32	32	31	31	31

(b)

LOWER RIGHT

79177-6

Figure 4. (a) 8 × 8 Pixel intensity map for star No. 237, in zoom, at position 5. (b) 8 × 8 pixel intensity map for star No. 125, in zoom, at position 1.

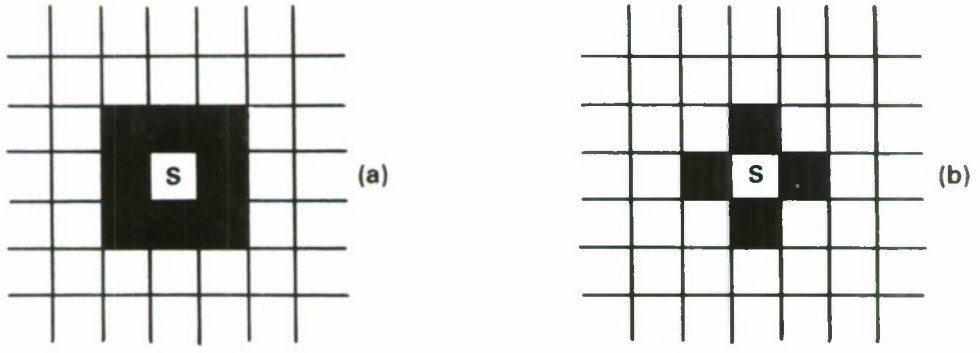

79177-7

Figure 5. (a). The definition of pixels included in "8-connected neighbors." The blackened pixels fulfill the meaning. (b) The definition of pixels included in "4-connected neighbors." The blackened pixels fulfill the meaning.

To do this rigorously requires an assumption about the underlying statistics of the amplitude levels and the presumption that μ_p, σ_p, μ_b, and σ_b are good estimators of their respective pixel distributions. The simplest, though slightly inaccurate, assumption concerning the underlying statistical distribution of the amplitude levels is that they are normally distributed. The only method to ensure that the sample statistics μ_p, σ_p, μ_b, and σ_b are good estimators for their population counterparts is to take as large a sample as possible. There are two separate concerns.

When the number of assigned star pixels is still small, then a 4-connected perimeter, as shown in Figure 5(b), will not have enough members to provide a good estimator of either the mean or the standard deviation about the mean. Therefore, if the total number of pixels assigned to the stellar category is less than or equal to 4, then the maximum perimeter (i.e., 8-connected) logic is used, otherwise the minimum (i.e., 4-connected) logic is used.

On the other hand, for bright stars, after the stellar region has grown significantly, the perimeter may encompass all the pixels originally assigned to the background category. This is an instance when the presence of the border, at the correct intensity level, provides an important simplification in the automation process.

Let us return to the case when $\mu_p > \mu_b$ by a statistically significant amount. Then we need to take at least one pixel from the (temporary) perimeter and permanently place it in the stellar category. Our first choice is the brightest perimeter pixel, if there is only one.

If there are two or more equally bright pixels in the perimeter, then their connectivity to the already-assigned stellar pixels is evaluated. We define connectivity to be the number of sides a perimeter pixel shares with a star pixel. Hence, connectivity is at most 4 and at least 0. Also, we add one-half to the connectivity of any perimeter pixel that trails along the row of the brightest pixel, or lies above and to its left, or below and slightly left, or straight down from it. The perimeter pixel to be permanently moved into the stellar category is the brightest pixel with the maximum connectivity.

If this discrimination fails, that is, if there are at least two equally bright, equally well-connected perimeter pixels, then we advance one more step. We calculate the distance of each of these pixels from the brightest stellar pixel. The closest one is eliminated from the perimeter. If it is still a toss-up, then we take all the brightest, best-connected, closest pixels from the perimeter and assign them to the stellar category.

After eliminating one or more pixels from the perimeter there is a new definition of the "star." We still have all the border pixels as just that, and the originally assigned background pixels are still so labeled. We form a new perimeter according to the above logic, recompute μ_p and σ_p, recalculate μ_b and σ_b, and ask all over again whether μ_p significantly exceeds μ_b. Eventually the answer will be no. When this happens all pixels that are not yet permanently assigned become background pixels.

There are now N pixels of the original 64 assigned to the star. To get the total background level B we sum the intensity levels over the remaining 64 – N pixels. The average background level is B/(64 – N). The star plus background level signal is contained in N pixels. Their intensity levels sum to S. Hence, starlight alone comprised an amplitude of S – NB/(64 – N), the numerator in Equation 1.

V. DATA ACQUISITION

Not knowing in advance how many pixels a star of a given magnitude would fill, we selected a subset of stars from the photographic photometry of Jones and Cudworth (1983) that spanned the likely range with the minimum spread in color index. The stars we actually used are listed in Table 1 along with their V, B-V, and computed m_{20} values.

Having arranged to perform the experiment in a small field of view and presumably being able to carry out the data acquisition rapidly, we did not attempt to do a rigorous estimate of the extinction. Nonetheless, one star was observed repeatedly (No. 118) as a real-time check. By looking at the variation in S – NB/(64 – N) for this star as a function of time and altitude, we could ascertain the state of the atmosphere. No significant degradation was detected.

Another consideration was to make sure that the stars were brought to the same location on the camera target in both fields of view, otherwise we would be comparing not only the zoom with the full-field but, inextricably intermixed, different places on the camera target. We already knew about the target's nonuniformity (see Figure 1). Both the presence of a grid on the operator's viewing monitor and the digital row and column indicators in the VICOM digital image processor helped to ensure the correct, repeated positioning. The errors are the largest for the brighter stars because their light falls over a larger area of the camera target.

There are several other factors that need to be incorporated into the observing procedures to ensure data quality. Some of these include keeping the gain setting constant throughout; allowing enough time for the camera electronics to stabilize when going from one configuration (zoom or full) to the other; minimizing the number of times that this is done; monitoring the state of the atmosphere for variable extinction; and signal averaging the one-thirtieth of a second video frame time over enough frames to ensure a good average but not so many that atmospheric turbulence can play a significant role.

Our observing sequence was star numbers 118, 237, 125, 185, 167, 148, 118, 237, 125, 185, 167, 148, and 118 again. Each star was observed first in the zoom mode, then in the full-field configuration. The full-field data for both 237 and 125 turned out to be contaminated by star light from a neighboring star to the east. Thus, these stars are not included in our results. This partial loss of information is another reason why we cannot reach a definitive conclusion concerning the relative sensitivities of the two fields of view. For the four remaining stars the signal-to-noise ratios for each field of view configuration are given in Tables 2, 3, and 4. The layout of the Tables corresponds to the data acquisition points in Figure 2 except the mean value for each field of view is in the central location. In a few instances the transfer of data from the digital image processor to the computer did not go well and we could not resurrect the intensity grids. Hence, there are a few blank entries in some positions.

TABLE 2

Signal-to-Noise Ratios for Star No. 118

First Pass

Z = 31.9 FF = 30.4	Z = 33.1 FF = 31.3	Z = 30.2 FF = 31.2
Z = 33.5 FF = 31.8	<Z> = 32.0 <FF> = 30.7	Z = 33.1 FF = 31.1
Z = 31.2 FF = 30.0	Z = 31.9 FF = 29.3	Z = 31.3 FF = 30.4

Second Pass

Z -- FF = 29.4	Z = 33.1 FF = 29.6	Z = 32.5 FF = 29.9
Z = 33.8 FF = 31.7	<Z> = 32.5 <FF> = 29.8	Z = 33.1 FF = 30.6
Z =30.2 FF = 28.4	Z = 32.1 FF = 29.1	Z -- FF = 29.6

Third Pass

Z = 30.1 FF = 28.2	Z = 31.7 FF = 29.2	Z = 31.5 FF = 30.3
Z = 31.8 FF = 30.1	<Z> = 30.9 <FF> = 29.3	Z = 32.1 FF = 30.9
Z = 29.6 FF = 28.1	Z = 30.4 FF = 28.1	Z = 30.0 FF = 29.2

Z = Zoom
FF = Full Field

TABLE 3

Signal-to-Noise Ratios of Stars — First Pass

Star No. 185		
Z = 5.67	Z --	Z = 5.94
FF = 7.02	FF = 6.32	FF = 7.04
Z = 6.74	<Z> = 6.20	Z = 7.12
FF = 6.73	<FF> = 6.46	FF = 6.76
Z = 5.78	Z = 6.07	Z = 6.11
FF = 5.45	FF = 6.62	FF = 5.72
Star No. 167		
Z = 4.12	Z = 4.16	Z = 3.83
FF = 3.96	FF = 4.67	FF = 4.09
Z = 4.49	<Z> = 4.02	Z = 4.30
FF = 3.79	<FF> = 3.93	FF = 4.19
Z = 3.79	Z = 4.17	Z = 3.29
FF = 3.41	FF = 3.74	FF = 3.60
Star No. 148		
Z = 2.31	Z = 3.04	Z = 2.24
FF = 1.91	FF = 2.34	FF = 2.25
Z = 2.57	<Z> = 2.47	Z = 2.39
FF = 2.96	<FF> = 2.37	FF = 2.99
Z = 2.73	Z = 2.61	Z = 1.85
FF = 1.72	FF = 2.50	FF = 2.27

Z = Zoom
FF = Full Field

TABLE 4

Signal-to-Noise Ratios of Stars — Second Pass

Star No. 185		
Z = 5.81	Z = 7.15	Z = 6.16
FF = 5.83	FF = 6.66	FF = 6.08
Z = 6.63	<Z> = 6.47	Z = 7.73
FF = 6.15	<FF> = 5.93	FF = 6.09
Z = 5.93	Z = 6.38	Z = 5.95
FF = 5.12	FF = 6.05	FF = 5.48
Star No. 167		
Z = 4.18	Z = 4.46	Z = 4.06
FF = 3.28	FF = 4.20	FF = 2.86
Z = 4.67	<Z> = 4.29	Z = 5.21
FF = 4.58	<FF> = 4.26	FF = 4.87
Z = 3.69	Z = 4.21	Z = 3.86
FF = 3.11	FF = 3.98	FF = 3.94
Star No. 148		
Z = 2.09	Z = 2.85	Z = 2.28
FF = 1.74	FF = 1.69	FF = 2.39
Z = 3.06	<Z> = 2.40	Z = 2.59
FF = 2.23	<FF> = 1.99	FF = 1.20
Z = 1.94	Z = 2.35	Z = 2.05
FF = 1.99	FF = 2.42	FF = 2.27

Z = Zoom
FF = Full Field

VI. RESULTS AND CONCLUSIONS

A study of Tables 3 and 4 shows a mixed set of results. Zoom vs full-field sensitivity depends on where one is on the camera target and on the intensity of the source. On the average, the zoom configuration produces a higher signal-to-noise ratio. Whether or not this corresponds to a half magnitude is less clear. The strongest conclusion this effort and other work of a similar nature (Yakutis, Taff, and Sayer, 1986) leads us to is that much needs to be done to adequately characterize cameras of this type.

ACKNOWLEDGMENTS

Support in performing this experiment was provided by Robert L. Irelan and Peter J. Trujillo. William J. Sahr provided the necessary software that enabled this experiment to proceed efficiently. Their assistance is greatly appreciated.

REFERENCES

1. B.F. Jones and K. Cudworth, Astron. J. **88**, 215 (1983).
2. J.M. Sorvari, "Magnitudes of Stars on the S-20 System," Project Report ETS-19, Lincoln Laboratory, MIT (1977), DTIC AD-A047099/7.
3. L.G. Taff, "The Analysis of Near-Earth Satellite Astrometric Data at the ETS," Project Report ETS-76, Lincoln Laboratory, MIT (1985), DTIC AD-A163902.
4. L.G. Taff, "The Completion of a Star Catalog for the Optical Aircraft Measurements Program," Technical Report 751, Lincoln Laboratory, MIT (1986), DTIC AD-A168017.
5. A.J. Yakutis, L.G. Taff, and S. Sayer, "Calibration of ETS Videotapes," Project Report ETS-77, Lincoln Laboratory, MIT (1986), DTIC AD-A168888.

REPORT DOCUMENTATION PAGE

1a. REPORT SECURITY CLASSIFICATION Unclassified	1b. RESTRICTIVE MARKINGS
2a. SECURITY CLASSIFICATION AUTHORITY	3. DISTRIBUTION/AVAILABILITY OF REPORT Approved for public release; distribution unlimited.
2b. DECLASSIFICATION/DOWNGRADING SCHEDULE	
4. PERFORMING ORGANIZATION REPORT NUMBER(S) ETS-78	5. MONITORING ORGANIZATION REPORT NUMBER(S) ESD-TR-87-014
6a. NAME OF PERFORMING ORGANIZATION Lincoln Laboratory, MIT 6b. OFFICE SYMBOL *(If applicable)*	7a. NAME OF MONITORING ORGANIZATION Electronic Systems Division
6c. ADDRESS *(City, State, and Zip Code)* P.O. Box 73 Lexington, MA 02173-0073	7b. ADDRESS *(City, State, and Zip Code)* Hanscom AFB, MA 01731
8a. NAME OF FUNDING/SPONSORING ORGANIZATION Air Force Systems Command, USAF 8b. OFFICE SYMBOL *(If applicable)*	9. PROCUREMENT INSTRUMENT IDENTIFICATION NUMBER F19628-85-C-0002
8c. ADDRESS *(City, State, and Zip Code)* Andrews AFB Washington, DC 20334	10. SOURCE OF FUNDING NUMBERS PROGRAM ELEMENT NO. 12424F; PROJECT NO. 292; TASK NO.; WORK UNIT ACCESSION NO.
11. TITLE *(Include Security Classification)* Zoom vs Full-Field Sensitivity at the ETS	
12. PERSONAL AUTHOR(S) Laurence G. Taff, Diane M. Jonuskis	
13a. TYPE OF REPORT Project Report 13b. TIME COVERED FROM _____ TO _____	14. DATE OF REPORT *(Year, Month, Day)* 1987 September 17 15. PAGE COUNT 30
16. SUPPLEMENTARY NOTATION	

17. COSATI CODES			18. SUBJECT TERMS *(Continue on reverse if necessary and identify by block number)*
FIELD	GROUP	SUB-GROUP	artificial satellites; video streaks; photometry; calibration

19. ABSTRACT *(Continue on reverse if necessary and identify by block number)*

This report discusses a formal attempt to quantify the zoom vs full-field sensitivities of the EBSICON cameras at the Experimental Test System of the Ground-based Electro-Optical Deep Space Surveillance (GEODSS) network. Our results are inconclusive due to lack of data. The hypothesis that the electronically zoomed configuration can reach approximately $0^{m}5$ fainter than the full-field mode neither can be confirmed nor denied on the basis of our work. More testing of these devices, and a wider variety of testing in general, is needed.

20. DISTRIBUTION/AVAILABILITY OF ABSTRACT ☐ UNCLASSIFIED/UNLIMITED ☒ SAME AS RPT. ☐ DTIC USERS	21. ABSTRACT SECURITY CLASSIFICATION Unclassified
22a. NAME OF RESPONSIBLE INDIVIDUAL Capt. Arthur H. Wendel, USAF	22b. TELEPHONE *(Include Area Code)* (617)863-5500, X-2330 22c. OFFICE SYMBOL ESD/TML